

Coherence of a charge density wave and phase slip in small samples of a quasi-one-dimensional conductor TaS₃

D. V. Borodin, S. V. Zaitsev-Zotov, and F. Ya. Nad'

Institute of Radio Engineering and Electronics, Academy of Sciences of the USSR, Moscow

(Submitted 16 February 1987)

Zh. Eksp. Teor. Fiz. **93**, 1394–1409 (October 1987)

Short samples of a quasi-one-dimensional conductor in the form of orthorhombic TaS₃ with submicron transverse dimensions exhibited a stepwise dependence of the electrical resistance on the electric field and temperature, with abrupt transitions between discrete metastable states. The current-voltage characteristics were highly nonlinear and exhibited a negative differential resistance region. The spectrum of narrow-band oscillations consisted of several narrow lines. These observations were attributed to a high degree of coherence of a charge density wave and to the appearance of stresses and strains in this wave under the influence of external forces. These stresses and strains were partly relieved by the process of phase slip activated both by thermodynamic fluctuations and by the electric field.

I. INTRODUCTION

Quasi-one-dimensional Peierls conductors such as transition metal trichalcogenides TaS₃, NbSe₃, and others similar to them exhibit a number of specific effects due to the existence of charge density waves (CDWs). Some of these effects had been observed some time ago, but until now their physical mechanism has not been fully understood. The problems under active discussion include the nonlinear contribution of CDWs to the conduction process,^{1,2} the form of current-voltage characteristics with switching³ and sometimes with a negative differential resistance region,⁴ metastable states and memory effects,^{1,2,5} narrow-band oscillation,^{1,2} etc. During the initial stage of the investigations of a number of features of these effects it had seemed that they could be explained by the concept of a rigid CDW moving as a whole. However, the subsequent more thorough investigations have made increasingly clear the need to allow for the deformability of CDWs and for the possibility of the existence of nonlinear excitations (solitons) in such a wave, and also of the interaction between CDWs and quasiparticle excitations (electrons and holes).

In addition both the theory and qualitative explanations of the experiments have begun to allow for the consequence of the existence in real crystals only of a short-range order in a CDW with finite amplitude ξ and phase l coherence lengths.^{6,7} Estimates of these lengths² show that they are much smaller than the dimensions of the samples of quasi-one-dimensional conductors usually employed. For example, in the case of orthorhombic TaS₃ estimates give the following values: the longitudinal correlation length is $\xi \approx 30$ Å, the longitudinal phase coherence length is $l \approx 10$ μm, and the transverse coherence length l_{\perp} is one or two orders of magnitude less.^{1,2,4,8,9} Therefore, a phase coherence region of length l_{\parallel} and diameter l_{\perp} is much less than the dimensions of the usually investigated samples which are $L \sim 1$ mm long and have $S \sim 10$ – 100 μm² cross sections. In other words, such large samples contain very large numbers ($\sim 10^6$) of phase coherence regions; the effects due to uncorrelated changes in the phase of individual phase coherence regions are then averaged out, so that the experiments reveal only the properties which are averaged over the volume of a sample.

In view of this situation it seemed desirable to investigate the effects due to the spatial inhomogeneity of a coherent CDW in samples, of small cross section and short length containing either a single phase coherence region or a small number of such regions. We discovered that, in the case of small samples, special features were exhibited by the temperature dependence of the resistance, current-voltage characteristics, current dependence of the differential resistance, and narrow-band generation of oscillations, and we also studied changes in the nature of these dependences when the transverse and longitudinal dimensions of the samples were altered. An analysis of these data revealed more clearly the physical nature of the effects due to coherent motion of a CDW.

II. EXPERIMENTS

1. Samples and experimental method

We investigated crystalline whisker samples of orthorhombic TaS₃ which were placed on insulating substrates (quartz, sapphire), with cross sections and lengths that varied over very wide ranges. Measurements were carried out on several dozen samples that could be divided arbitrarily into three groups: group 1 comprising samples with transverse dimensions 1–10 μm (of $S = 1$ – 100 μm² cross section) and with lengths of the investigated regions (sections) between contacts within the range 300–1000 μm; group 2 consisting of samples with transverse cross sections 0.1–1 μm²; group 3 representing the thinnest samples with cross sections 10^{-1} – 10^{-3} μm².

Contacts were formed by evaporation of several (up to six) narrow (≈ 10 μm) metal strips separated by distances $L = 5$ – 1000 μm (Refs. 2, 10, 11). The dimensions of the samples were deduced from their room-temperature resistance, by optical methods, and also with the aid of an electron microscope.¹¹ Table I lists the dimensions of the investigated samples and their principal parameters. The initial thick samples (10–100 μm²) were used to prepare thin samples and they were quite pure with a threshold field $E_T \approx 0.25$ V/cm ($T = 120$ K) and a three-dimensional ordering temperature $T_p = 225$ K. We determined the temperature dependence of the resistance $R(T)$, the current-voltage

TABLE I.

Group No.	Sample No.	Cross-sectional area, μm^2	Section length, μm					E_T , V/cm	T_p , K
			a	b	c	d	e		
1	1	66	1160	—	—	—	—	0.27	225
	2	24	365	—	—	—	—	0.43	219
	3	11	365	—	—	—	—	0.47	—
2	4	0.7	75	40	55	120	310	0.9	—
	5	0.6	27	50	225	360	790	0.8	220
	6	0.5	5	27	45	120	290	1.8	218
	7	0.35	23	90	120	155	—	1.0	—
	8	0.3	45	—	—	—	—	1.7	—
	9	0.15	30	105	280	—	—	1.2	220
	10	0.033	24	—	—	—	—	3.5	211
3	11	0.02	24	—	—	—	—	5.3	209
	12	0.017	8	24	—	—	—	8.5	198
	13	0.008	24	114	—	—	—	5.0	208
	14	0.005	6	24	—	—	—	11	198

characteristics, the current dependence of the differential resistance $R_d(I)$, and also spectra of narrow-band oscillations. Measurements were carried out using a circuit with a high noise immunity, which made it possible to determine the resistance of thin high-resistance samples under constant-current conditions when the amplitude of modulation of the current was less than 1% of the threshold current I_T (Ref. 10).

2. Temperature dependence of the resistance

The temperature dependence of the resistance $R(T)$ recorded in the range 300–77 K for group 1 samples were of the usual form with a steep rise of the resistance near $T \approx T_p$ and a smooth activated region (200–100 K) with a slope corresponding to an energy $\Delta \approx 800$ K (Ref. 12). The $R(T)$ curve obtained during cooling was located below the curve recorded during heating, i.e., hysteresis was observed in the range 200–77 K (Ref. 13). The dependence $R(T)$ for group II samples was similar to the corresponding dependence for thick group 1 samples, except that in the case of the thinnest samples there was a small reduction in T_p and some broad-

ening of the abrupt transition at $T \approx T_p$. These changes were manifested most strongly in the shortest ($L \approx 10 \mu\text{m}$) samples.⁴ Further reduction in the cross section of the samples (group 3) reduced T_p more strongly. Figure 1 shows the temperature dependence of the logarithmic derivative of the curves $R'(T) = d \lg(R/R_{300})/d(10^3/T)$ obtained for several samples of different cross sections S (the maxima of these curves occurred at $T = T_p$). Beginning at $S \approx 0.1 \mu\text{m}^2$ the $R'(T)$ curves shifted toward lower temperatures, became broader, and the maxima decreased. In the case of samples with $10^{-3} < S < 1 \mu\text{m}^2$ cross sections these results were obtained mainly for sections of $L \gtrsim 25 \mu\text{m}$ length. In the case of the shortest sections ($L < 10 \mu\text{m}$) we observed a further broadening of the maxima of the $R'(T)$ curves and a reduction in T_p (samples 12a and 14a in Fig. 1). It is clear from the general dependence $T_p(S)$ (inset in Fig. 1) that the reduction in T_p reached ~ 30 K.

The most important qualitatively new feature of the $R(T)$ dependence on reduction in the cross section was the appearance of a step structure.¹⁰ The relative amplitude of the steps of the $R(T)$ curve increased as S was reduced (group 2). In group 3 samples with the $10^{-1}-10^{-2} \mu\text{m}^2$ cross sections this step structure became dominant.

Figure 2 shows the $R(T)$ dependence for sample 11 when it was cooled from 120 to 90 K and heated again. This curve exhibits hysteresis and it consists of short, almost linear, regions with a slope $d(\ln R)/d(1/T) \approx 200$ K smaller than the activation energy $\Delta \approx 800$ K of conduction in thick samples. Within these regions the resistance $R(T)$ varied smoothly, but the transitions between them are discontinuous. The steps occur in a time shorter than the time constant of the measuring circuit (0.3–1 s). The relative change in the resistance at a step was $\Delta R/R = 1-10\%$. The magnitude ΔR of the steps and the distance ΔT between them were functions of temperature and became smaller when the sample temperature was increased. In group 3 samples the steps of $R(T)$ were clearly distinguishable up to temperatures ~ 180 K. The change in the resistance at a step was always directed inside the hysteresis loop. Repeated measurement of the dependence shown in Fig. 2 established that the temperatures at which the steps occurred fluctuated somewhat. The regions of smooth variation of R between the steps were readily reproducible, stable, and hysteresis-free. We include in Fig. 2 (inset) a detailed sequence of variation of R , labeled

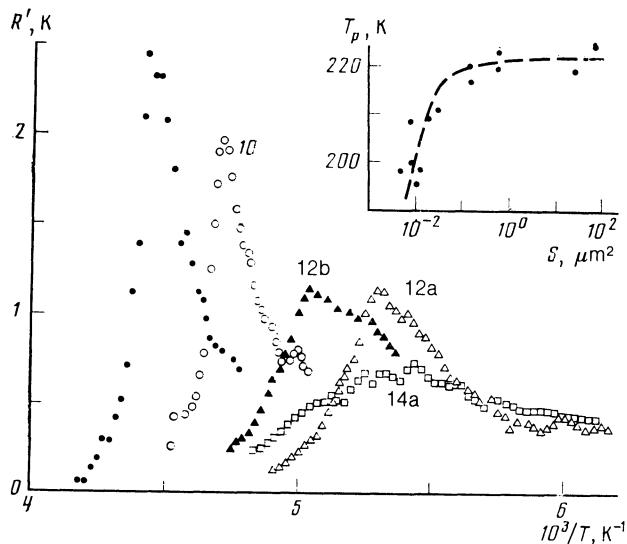


FIG. 1. Temperature dependence of the logarithmic derivatives of the resistance of small samples. The numbers alongside the curves give the numbers of samples used in Table I. The inset shows the dependence of the three-dimensional ordering temperature T_p on the cross section of a sample.

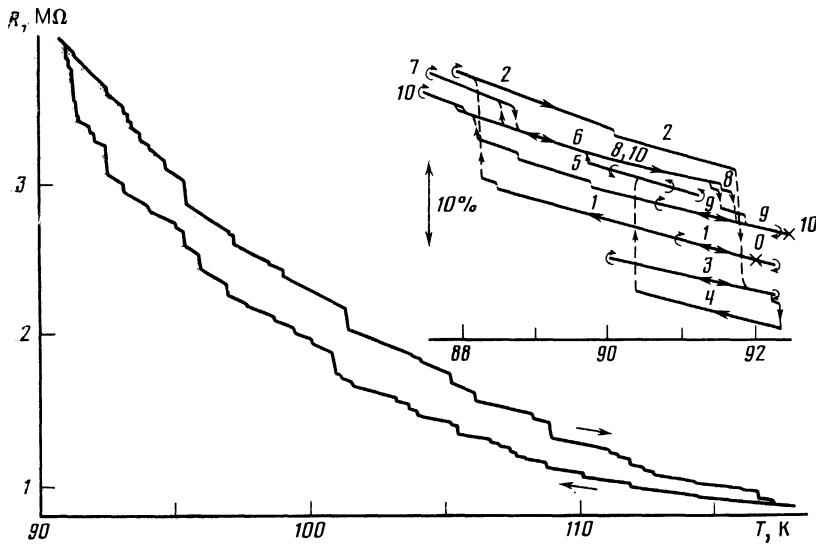


FIG. 2. Temperature dependence of the resistance R of a group 3 sample (sample 11). The inset is a fragment of the dependence $R(T)$ obtained in the course of temperature cycling in the range 88–92 K. The numbers in this inset identify the sequence of changes in R [the crosses correspond to the beginning (0) and end (10) of the record].

by numbers, in the course of cyclic variation of the temperature of the sample in the range 88–92 K. Clearly, the resistance of the sample changed abruptly between discrete states which were separated by approximately the same values of R ($\Delta R/R \approx 4\%$). In some cases during the process of temperature cycling a sample frequently reached the state with the same value of R (states 6, 8, 10). The change of R in any one of the states (after a step) was smooth and almost linear for both temperature increases and decreases within certain limits $\Delta T = 2\text{--}5$ K. In these regions we observed no hysteresis of the $R(T)$ curve, within the limits of the experimental error ($\sim 0.3\%$). It should be mentioned that in the case of thick samples the dependence $R(T)$ during cycling within the same interval 5 K exhibited a strong hysteresis which was retained down to the smallest temperature intervals $\Delta T \leq 0.2$ K.

In the case of ultrathin samples with cross sections $S < 10^{-2} \mu\text{m}^2$ we observed a reduction in the hysteresis and narrowing of the temperature range in which it occurred (hysteresis began at lower temperatures), the steps became less clear, and their amplitude decreased somewhat. This

tendency was manifested most clearly by the shortest samples ($L < 10 \mu\text{m}$).

3. Dependence of the resistance on the electric field

We also investigated the dependence of the shape of the current-voltage characteristics near the threshold field on the cross section S of a sample when S was varied over four orders of magnitude (from 10^{-2} to $10^2 \mu\text{m}^2$). In the case of long samples a reduction of the cross section from $S > 10 \mu\text{m}^2$ (group 1) to $S < 0.1 \mu\text{m}^2$ altered qualitatively the initial parts of the current-voltage characteristics. Figure 3 shows a series of typical dependences of the conductivity $\sigma = I/U$ on the electric field $E = U/L$ obtained for samples of different cross sections. It can be seen that in the case of group 1 samples (samples 1 and 2) an increase in the field in the range $E > E_T$ resulted in a smooth increase of the conductivity, usually attributed to incoherent motion of a deformable CDW.¹⁴ In group 2 samples (samples 5 and 9) an increase in the conductivity with the field E became even steeper. As shown earlier,⁴ the thinnest group 2 samples exhibited a region with a positive curvature $d^2U/dI^2 > 0$, near the threshold field and in some cases at temperatures $120 < T < 140$ K there was a negative differential resistance region. These effects were evidence of an increase in the coherence of a CDW in group 2 samples and indicated that these samples were close to the characteristic phase coherence lengths.¹⁵ As the cross section of the samples decreased, the region with a positive curvature broadened, so that in the case of the thinnest sample for which the shape of the current-voltage characteristics was investigated a fourfold increase in the conductivity was observed for a practically constant voltage across a sample (sample 13b in Fig. 3). It is clear from Fig. 3 that the threshold field E_T for the appearance of nonlinear conduction increased by more than one order of magnitude when the cross section of the samples was reduced from 10^2 to $10^{-2} \mu\text{m}^2$. The dependence $E_T(S)$ is shown in Fig. 3 (inset). In the range $S < 1 \mu\text{m}^2$ the field obeyed $E_T \approx V_s S^{-1/2}$, where $V_s \approx 0.1$ mV. The scatter of the experimental data on the $E_T(S)$ plot was clearly due to the different shapes of the transverse cross sections of the investigated samples.

We also found that the resistance of group 3 samples

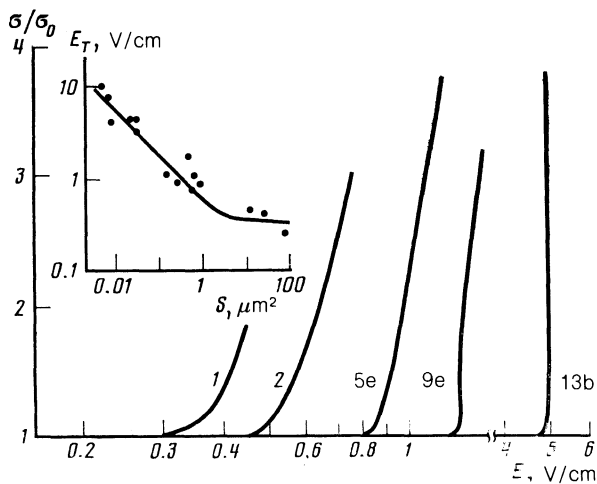


FIG. 3. Conductivity, normalized to its value σ_0 when $E < E_T$, versus the electric field applied to samples of different cross sections. The numbers alongside the curves identify the sample number. The inset gives the dependence of the threshold field E_T on the cross section S of the samples ($T = 120$ K).

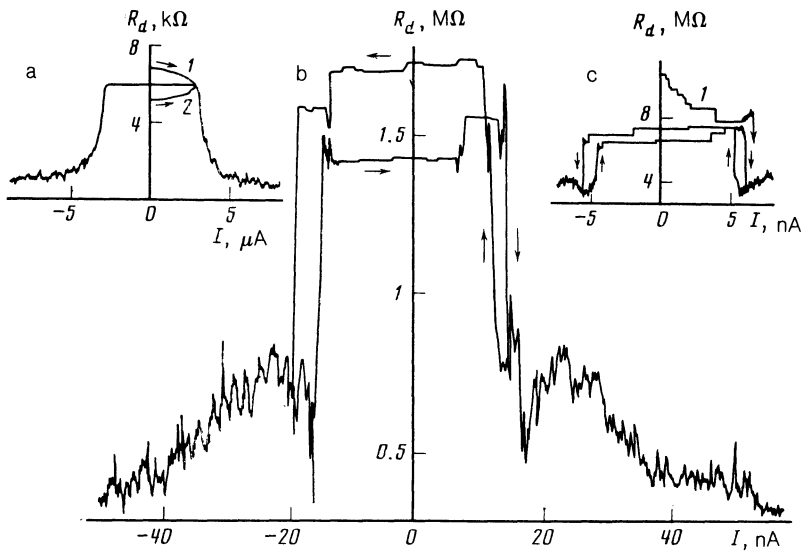


FIG. 4. Dependence of the differential resistance on the current: a) sample 2, $T = 120$ K; b) sample 11, $T = 98$ K; c) sample 14b, $T = 98$ K.

changed discontinuously when the current was altered in the range $|I| < I_T$. This effect was manifested most clearly in the dependence of the differential resistance R_d on the current I in short samples ($L \approx 25 \mu\text{m}$), as shown in Fig. 4. When the sample was initially in a metastable state, governed by the previous thermal history, the first increase of the current suppressed the metastable state abruptly (curve 1 in Fig. 4c) and not smoothly,⁵ in contrast to a group 1 sample (curves 1 and 2 in Fig. 4a). Repeated measurement of the dependence $R_d(I)$ showed that it exhibited reproducible hysteresis with small fluctuations in the switching times at $I \approx I_T$ (Figs. 4b and 4c). A specific feature of the small TaS₃ samples we investigated was the abrupt nature of the changes in the differential resistance when the current was varied.

It had been shown earlier⁴ that a reduction of the length of group 2 samples ($S \approx 1 \mu\text{m}^2$) to $L < 100 \mu\text{m}$ reduced the nonlinearity of the current-voltage characteristics and broadened the sharp inflection of the characteristics near $I \approx I_T$. This was attributed to an increase in the inhomogeneity of the electric field near the current contacts, which could be described by a geometric factor $X = (SA)^{1/2}/L$ (A is the conductivity anisotropy); when the length of these samples was $L \approx 20 \mu\text{m}$, it satisfied $X \sim 1$. In the case of the thinnest group 2 samples and in group 3 samples the geometric factor was almost an order of magnitude less, the region with an inhomogeneous electric field at the contacts was small, and it did not prevent a strong nonlinearity of the current-voltage characteristics near $E \gtrsim E_T$ (Fig. 3).

In addition to an increase in E_T , we found that group 2 samples exhibited also a nontrivial increase in the threshold current as the length of the sample decreased.⁴ One can show (as is done later in Sec. III) that an investigation of the dependence $I_T(L)$ rather than the dependence $E_T(L)$, as in Ref. 4, demonstrated effects associated with conversion of a CDW current into a current of quasiparticles even when the electric field varied rapidly near the contacts. With this in mind we investigated the dependence $I_T(L)$ for several group 2 samples. Figure 5 displays the threshold current I_T normalized to I_t in the longest section as a function of the section length L .

Clearly, a reduction of the distance between the con-

tacts increased the threshold current I_T : $I_T \approx I_t(I/L + 1)$, where in the case of the samples with cross sections in the range $0.1\text{--}1 \mu\text{m}^2$ we had $\sim 10\text{--}20 \mu\text{m}$ at $T = 120$ K.

The ratio of the threshold currents in long and short sections was found to depend strongly on temperature (inset in Fig. 5). In the temperature range $150\text{--}180$ K the difference between the values of I_T in short and long samples was less than the experimental error. When the temperature was lowered, the difference between the threshold currents in long and short sections increased. At the same time, the nature of the temperature dependences of the threshold field was different for long and short sections. When a sample was shortened, the minimum of the dependence $E_T(T)$ became less pronounced^{2,16} and in the case of the shortest samples the minimum disappeared almost completely.

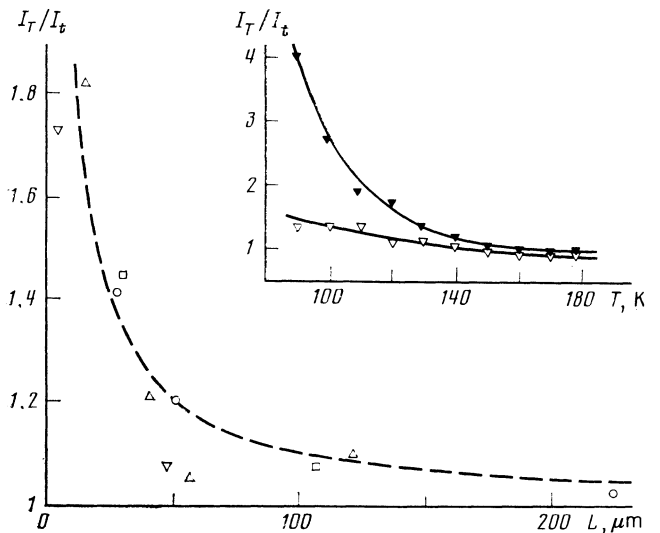


FIG. 5. Dependence of the threshold current I_T on the length of a section L in various samples. The value of I_T is normalized to the threshold current I_t of the longest section in each sample. The dashed curve is the dependence $I_T(L)$ calculated on the basis of Eq. (8) for $V_{ps} = 1$ mV and $E_c = 1$ V/cm. The inset shows the temperature dependences of I_T/I_t for sections a (\blacktriangledown) and c (\triangledown) of sample 6.

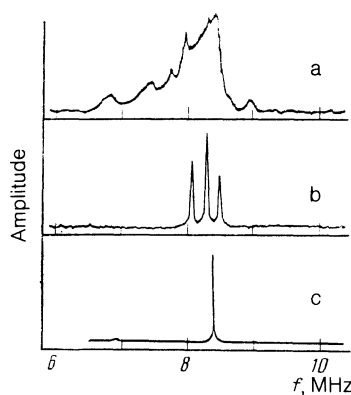


FIG. 6. Profiles of narrow-band oscillations generated in samples of different cross sections: a) sample 2; b) sample 8; c) sample 10.

4. Generation of periodic oscillations

Information on the coherence of the motion of a CDW can also be obtained by investigating narrow-band oscillations. We found that as the thickness of the samples varied the profile and width of the narrow-band oscillation lines varied considerably. The lines in the oscillation spectrum of group 1 samples had an irregular profile and relatively large width $\Delta f \sim 1$ MHz (Fig. 6a). When the cross section of the samples was reduced, the fundamental line seemed to split into several narrow lines. In the case of the thickest group 2 samples there were several fundamental lines of width ~ 100 kHz, each with its own harmonics.

A further reduction in the size of the sample reduced the number of the fundamental lines and their width. In the case of the thinnest group 2 samples we observed a small number of the fundamental lines with width $\Delta f < 100$ kHz (Fig. 6b). The spectrum of some of these samples consisted of a single fundamental line of width less than 10 kHz at $T = 120$ K (Fig. 6c). In this case the wide-band $1/f$ noise was weak compared with the noise in thick samples and narrow-band oscillations were observed beginning from low frequencies in the range $f \approx 50$ kHz. The current-voltage characteristics of these samples had a strong inflection at $I \approx I_T$. In the case of group 2 samples an increase in temperature increased the width of the oscillation lines and at temperatures $T > 150$ – 170 K the narrow-band oscillation line disappeared in the wide-band noise background. When the cross section of the samples was reduced to $S \sim 10^{-2} \mu\text{m}^2$ narrow-band oscillation lines began to smear out. In the thinnest samples ($S < 10^{-2} \mu\text{m}^2$) at currents in the range $I > I_T$ only low-frequency noise with spectral density $f^{-\alpha}$ ($\alpha \sim 1$) was observed and there were no narrow-band oscillation lines.

III. DISCUSSION

As pointed out in the Introduction, the properties of quasi-one-dimensional conductors are influenced strongly by the internal degrees of freedom of a coherent CDW and also by deformation of the wave and nonlinear excitations (including solitons) in the wave. Our investigation of relatively pure samples with small cross sections and short lengths made it possible to approach a situation when a CDW was coherent throughout the sample. This allowed us to observe directly the effects due to the above-mentioned features of CDWs.

Our study and earlier investigations^{4,10,17} provided much experimental evidence in support of the existence of coherent CDWs in small TaS₃ samples. A reduction in the cross section and the length of the samples reduced considerably the smearing of the current-voltage characteristic near $E \approx E_T$ and made the inflection sharper (Fig. 3); a negative differential resistance⁴ was observed, which was typical of coherent CDWs.^{15,18} The temperature dependence of the resistance of small samples clearly revealed hysteresis-free regions and abrupt transitions between them (Fig. 2), which were hard to observe in large samples because these features were averaged over the volume of the sample containing a large number of uncorrelated phase coherence regions. An increase in the degree of coherence of a CDW in our samples was manifested also by changes in the nature of the spectra of narrow-band oscillations: the number of the fundamental oscillation lines decreased right down to one and the lines became much narrower (Fig. 6).

However, it should be pointed out that electron diffraction investigations showed⁹ that the longitudinal coherence length of a CDW in TaS₃ (obtained when a beam of electrons interacted with a sample) was less than $1 \mu\text{m}$, i.e., it was less than the length of our samples. The fact that we were able to observe effects due to a coherent CDW clearly indicated that when a small number of phase coherence regions were present in a sample the coherence effects were still retained throughout the sample or these regions could behave in a phase-matched (coherent) manner.²

A further reduction in the length of TaS₃ samples (in our case to $L < 10 \mu\text{m}$) did not improve the situation, because even in the thinnest samples the effects of an inhomogeneity of the electric field near the contacts became significant.⁴ A reduction of the cross sections to values less than $10^{-2} \mu\text{m}^2$ also clearly did not improve the coherent behavior of a CDW, since in such samples the role of three-dimensional effects became weaker and the influence of fluctuations, sample surfaces, and blocking effects of impurities became stronger. This was indicated by broadening of the dependence $R(T)$ we observed for these samples near the temperature T_p , by a considerable reduction in T_p (Fig. 1), and by weakening of the step structure and a strong rise of the threshold field (Fig. 3). Therefore, in our case (orthorhombic TaS₃) the optimal cross sections and lengths for the observation of coherent effects were near $S = 10^{-1}$ – $10^{-2} \mu\text{m}^2$ and $L = 10$ – $100 \mu\text{m}$, respectively. An increase in the purity of the material and of its structural quality should make it possible to observe similar effects also in samples with larger dimensions.

Bearing these points in mind, we shall discuss a model of a CDW and its deformation in small samples assuming, for the sake of simplicity, that this wave is coherent throughout the sample. It is known that in many quasi-one-dimensional materials, including orthorhombic TaS₃, a CDW is incommensurate with the original lattice and this is true in a wide range of temperatures $T < T_p$ (Refs. 2 and 19). In view of its rigidity, the original crystal lattice and its wave vector are practically unaffected by externally electric fields and temperatures. Since a CDW is much "softer," its wave vector q responds much more sensitively to external influences and exhibits greater changes. In particular, this is true of an incommensurate CDW in which deformations and nonlin-

ear excitations are obviously most likely. Experimental studies have established that, for example, in the case of orthorhombic TaS₃ at temperatures 100–200 K the transverse and longitudinal components of q vary during cooling by about 2% approaching the commensurate situation, so that below 100 K the value of q corresponds to a fourfold commensurability.¹⁹ Direct measurements on a quasi-one-dimensional conductor K_{0.3}MoO₃ have also revealed a change in q (by a few percent) under the action of an electric field.²⁰

In describing the electronic properties of a small sample we shall find it sufficient to consider such a sample as a system consisting of two interacting subsystems: a CDW and quasiparticles. It is important to note that if the CDW departs at all from thermodynamic equilibrium because of the condition of electrical neutrality,²¹ the properties of the quasi-one-dimensional sample governed by the quasiparticles, for example, the electrical conductivity of the sample in the range of fields $E \gg E_T$, are altered. It is convenient to describe these changes in terms of a shift of the chemical potential level of quasiparticles ζ (Refs. 10, 22, and 23), which is a consequence of the appearance of elastic "stresses" and strains in a CDW and of the associated excess charge. For example, a shift of the chemical potential $\delta\zeta$ in the case of inhomogeneous deformation of a CDW is proportional to the gradient of the CDW phase $d\varphi/dx \sim \delta q \ll q$. The change in the Peierls gap then depends quadratically on $d\varphi/dx$ and is negligible for $\zeta \ll \Delta$ (Ref. 23). These stresses and strains are reversible only if δq is small. If large deformations exceed a certain threshold value, a stepwise local change in the phase of a CDW by an amount which is a multiple of 2π and relieves the accumulated strain if favored.^{23,24}

The main features of these effects can be described by fairly simple phenomenological relations in the simplest one-dimensional model of a Peierls conductor with a coherent CDW. An additional charge due to the deviation of a CDW and its wave vector q from the value q_0 governed by the total number of electrons per unit length of one chain, $n_0 = q_0/\pi$, is balanced by the corresponding change in the densities of quasiparticles, both electrons (n) and holes (p):

$$n_0(q - q_0)/q_0 + n = p. \quad (1)$$

In the case of weakly interacting chains this relationship applies also to the corresponding volume densities, obtained by multiplying the linear densities by the number of filaments per unit cross section. The densities n and p can be expressed in terms of the effective densities of states N_n and N_p , which for the sake of simplicity will be assumed to be the same ($N_n = N_p = N$):

$$n = N \exp[-(\Delta - \zeta)/T], \quad p = N \exp[-(\Delta + \zeta)/T],$$

where ζ is the chemical potential level measured from the middle of the Peierls gap. Then, Eq. (1) yields

$$n_0(q - q_0)/q_0 = -2Ne^{-\Delta/T} \operatorname{sh}(\zeta/T). \quad (2)$$

This equation determines the relationship between ζ and q . The conductivity of a quasi-one-dimensional conductor in a weak field below the threshold value, $E < E_T$, is governed by quasiparticles:

$$\sigma = en\mu_n + ep\mu_p,$$

where μ_n and μ_p are the mobilities of electrons and holes,

respectively. If, for the sake of simplicity we assume that $\mu_n = \mu_p = \mu$, we find that

$$\sigma = 2e\mu N e^{-\Delta/T} \operatorname{ch}(\zeta/T). \quad (3)$$

We shall now analyze the stepwise temperature dependence of the resistance of small samples $R(T)$ (Fig. 2) using Eqs. (2) and (3). In a given temperature interval $\Delta T \sim 1$ K between jumps a CDW is in a metastable states with a certain constant value of q , which differs from q_0 because the thermodynamic equilibrium value of q_1 depends on T (Ref. 19). In a sample with the CDW phase pinned at the contacts these states correspond to a set of discrete values of the wave vector $q \approx q_m = 2\pi m/L$ of a CDW. Since variation of temperature within this interval does not alter the value of q , the dependence $R(T)$ remains hysteresis-free. It is clear from Eq. (2) that if $q - q_0 = \text{const}$ the chemical potential level ζ depends strongly on T . This dependence of ζ reflects the appearance of an internal homogeneous reversible stress in a CDW and a corresponding change in the free energy of the electron subsystem. A further change in temperature beyond the interval ΔT results in a transition to a new metastable state because of an abrupt change by 2π in the difference between the phases of CDW at the ends of a sample, i.e., because of the appearance or elimination of a new CDW period.

It is clear from Fig. 2 that hysteresis-free regions between the steps are characterized by an activation energy ε^* smaller than Δ , which corresponds to the average dependence $\sigma(T)$ without allowance for the steps. The activation energy of the conduction process $\varepsilon = d \ln \sigma / d(1/T)$ is given by the following expression which is derived from Eq. (3) for a constant value of Δ :

$$\varepsilon = \Delta - \operatorname{th} \frac{\zeta}{T} d\left(\frac{\zeta}{T}\right) / d\left(\frac{1}{T}\right) \quad (4)$$

(we are ignoring the weak temperature dependence of μ and N). It follows from Eq. (4) that the activation energy of conduction ε depends on the position of the chemical potential level and on its rate of change with temperature. In its turn the chemical potential level is related to the wave vector of a CDW in accordance with Eq. (2). In the region between the steps when $q - q_0 = \text{const}$, we have

$$d\left(\frac{\zeta}{T}\right) / d\left(\frac{1}{T}\right) = \Delta \operatorname{th} \frac{\zeta}{T}$$

and the activation energy of conduction becomes in this region

$$\varepsilon^* = \Delta [1 - \operatorname{th}^2(\zeta/T)] = \Delta / \operatorname{ch}(\zeta/T). \quad (5)$$

This relationship allows us to estimate the shift of the chemical potential level. Using the experimental value $\varepsilon^* = 200$ K (Fig. 2) and assuming that $\Delta = 800$ K, we obtain $-\zeta/T \approx 1.3$ [the sign of $\zeta < 0$ follows from Eq. (2) when $q - q_0 > 0$, which corresponds to orthorhombic TaS₃ (Ref. 19)]. Therefore, the chemical potential level of orthorhombic TaS₃ at $T \sim 100$ K is shifted downward by $\approx kT$ relative to the middle of the gap. This result is in good agreement with the experimental investigations of the thermoelectric power^{22,25} and of the Hall effect,²⁶ and with the distribution of the equilibrium values of the resistance within a temperature hysteresis loop^{5,27} [see Eq. (2)].

As already mentioned, the transition to the next meta-

stable state due to variation of temperature may occur when a fixed value of q deviates from the thermodynamic equilibrium q_1 by an amount $\delta q = 2\pi/L$. Knowing the experimental dependence $q_1(T)$ averaged over a large sample,¹⁹ we can estimate the temperature interval between the steps: $\Delta T = \delta q(dq_1/dT)^{-1}$. Substitution of the experimental data from Ref. 19 gives $\Delta T \sim 1$ K, which is in good agreement with our value of ΔT (Fig. 2). This can be regarded as a confirmation of the assumption that stepwise changes in the resistance occur as a result of creation (or annihilation) of a new CDW period in a sample, i.e., due to a change in q by $\delta q = 2\pi/L$. According to Eqs. (2) and (3), the conductivity of a sample can be described by

$$\sigma = en_0\mu[(q - q_0)/q_0] \operatorname{cth}(\xi/T). \quad (6)$$

For $|\xi/T| > 1$, it follows from Eq. (6) that $\delta\sigma/\sigma \approx \delta q/(q - q_0)$. In the case of a sample of length $L = 20 \mu\text{m}$ for $q - q_0 = 2 \times 10^3 q_0$ at $T = 200$ K (Ref. 19), we obtain $\delta\sigma/\sigma \sim 3\%$, which is in satisfactory agreement with the experimental results (Fig. 2). Therefore, the appearance (or disappearance) of a new CDW period in a sample, corresponding to the appearance of a charge $2e$ on each chain, may be detected from a change in the resistance of a small sample by an easily measurable amount $\sim 10\%$, whereas the corresponding change in the wave vector of a CDW is small: $\delta q/q_0 \sim 10^{-4}$. The inset in Fig. 2 demonstrates also that at a given temperature (for example, near 90 K) a real sample contains several metastable states and the transition takes place not only to the nearest but to one of the other adjacent states (regions 4 and 2).

Similar stepwise transitions between metastable states partly or completely relieving the stresses or strains in a CDW occur also at a constant temperature when the current I is increased, including the range of currents smaller than the threshold value I_T (Fig. 4c). In other words, an external electric field acts like a change in temperature on a CDW facilitating transitions between metastable states.

What is the physical mechanism of the step itself? Such observations as the relationship between the steps and the deformation of a CDW, the considerable influence of temperature and of the electric field, and the change in the phase of a CDW by an amount which is a multiple of 2π suggest that the observed steps are most probably due to the formation of a local phase slip center.^{23,24,27-29} Both theoretical^{23,24,27} and experimental²⁷ studies of phase slip centers have been made mainly on the assumption that these centers are responsible for converting a current of quasiparticles into a CDW current and for the generation of narrow-band noise in a CDW near the contacts in a quasi-one-dimensional conductor. It is also assumed that the presence of a phase slip center should be manifested in the time-averaged current-voltage characteristics of a quasi-one-dimensional conductor by an additional voltage V_{ps} which is regarded as responsible for the rise of the threshold field E_T when the length of the conductor is reduced.^{30,31} However, since the majority of the earlier investigations have been carried out on fairly thick samples with transverse dimensions $\sim 1-10 \mu\text{m}$, the strong anisotropy A of the conductivity could result in the formation of regions with an inhomogeneous electric field near the contacts of size $(SA)^{1/2}$ reaching $10-100 \mu\text{m}$. This makes it difficult to establish reliably the existence of V_{ps} ,

although some confirmations of this fact are available particularly in the case of NbSe_3 (Ref. 2). By using samples of transverse dimensions $\sim 0.1 \mu\text{m}$ and of length $\sim 10 \mu\text{m}$ in our study reduced considerably the influence of the inhomogeneity of the electric field and enabled us, as shown below, to confirm reliably the existence of V_{ps} and, consequently, of phase slip centers in small TaS_3 samples and to determine their main characteristics. Similar results were recently reported for NbSe_3 (Ref. 29).

The shape of the current-voltage characteristic of a quasi-one-dimensional conductor is governed by two contributions associated with the dissipation of energy in its interior due to the motion of quasiparticles and of a CDW as well as with the process of conversion of a CDW current into a current of quasiparticles. Such a conductor can be represented by an equivalent circuit shown in Fig. 7. According to this equivalent circuit, the current-voltage characteristic of such a conductor can be written in the form

$$U = 2r_i I + V_{ps}(I_c) + E_c(I_c)L, \quad (7)$$

where

$$V_{ps}(I_c) + E_c(I_c) = \rho L I_q$$

(the notation is explained in the caption of Fig. 7). If we define the threshold current I_T as the current corresponding to some maximum CDW current found experimentally, $I_c \ll I_T$, we obtain the dependence of I_T on the length of the sample:

$$I_T = V_{ps}(I_c^*)/\rho L + E_c(I_c^*)/\rho. \quad (8)$$

It should be noted that the dependence $I_T(L)$ of Eq. (8) does not include, in contrast to $E_T(L)$, the spreading resistance r_i ; the rise of I_T as L decreases, which is then predicted, can be regarded as clear evidence of the existence of V_{ps} . The dependence $I_T(L)$ of Eq. (8) corresponding to $V_{ps} = 1$ mV and $E_c = 1$ V/cm is represented by a dashed curve in Fig. 5. The good agreement between the calculated [Eq. (8)] and experimental dependences is one of the proofs of the existence of the time-averaged voltage $V_{ps} \approx 1$ mV ($T = 120$ K) due to the processes of phase slip at the contacts of a sample.

It is possible to identify the contribution V_{ps} and to determine its dependence on I_c and temperature from the current-voltage characteristics $U_1(I_1)$ and $U_2(I_2)$ obtained for sections of different lengths L_1 and L_2 in the same sample:

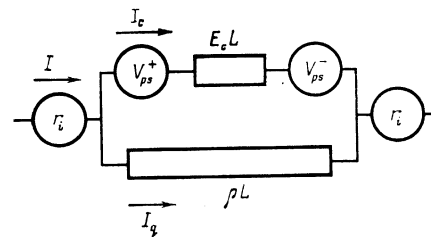


FIG. 7. Equivalent circuit of a sample of a quasi-one-dimensional conductor with a coherent charge density wave. Here, L is the length of the sample, ρ is the resistance per unit length in the case when $I < I_T$, r_i is the "spreading" resistance,⁴ $E_c(I_c)$ is the electric field corresponding to the current I_c and to the motion of a charged density wave in the field of pinning forces in the bulk of a sample, V_{ps}^+ and V_{ps}^- are the voltage drops associated with the conversion of a charged density wave current I_c into a quasiparticle current I_q .

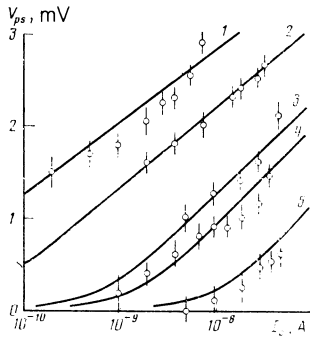


FIG. 8. Dependence of V_{ps} on the charge density wave current I_c plotted for different temperatures of sample 9. The continuous curves were calculated from Eq. (10) on the assumption that $I_0 = 3.5$ A, $F = 1500$ K, $\eta = 60e$. The dependences were recorded at the following temperatures (K): 1) 100; 2) 111; 3) 128; 4) 134; 5) 151.

$$V_{ps}(I_c) = [(U_1 R_2 - U_2 R_1) / (R_2 - R_1)] (1 + \alpha) - \beta, \quad (9)$$

where R_1 and R_2 are the resistances of the sections when $I < I_T$, and α and β are small ($\sim 1\%$) corrections associated with the presence of r_i :

$$\alpha = 2r_i/R_1 + 2r_i/R_2 + (2r_i)^2/R_1 R_2, \quad \beta = 2r_i I_c.$$

In Eq. (9) we shall use the voltages U_1 and U_2 corresponding to the same CDW current $I_c = (I - U/R)/(1 - \gamma)$ where $\gamma = 2r_i/R$ is a small correction. The error in the determination of V_{ps} was reduced by determining the dependences $V_{ps}(I_c)$ for thin samples with transverse dimensions $\sim 0.1 \mu\text{m}$ and with current-voltage characteristics corresponding to a CDW coherent through the whole volume of the sample. Figure 8 shows a typical series of dependences $V_{ps}(I_c)$ obtained at different temperatures from the current-voltage characteristics of two sections of lengths $L_1 = 30 \mu\text{m}$ and $L_2 = 105 \mu\text{m}$ in sample 9. It is clear from Fig. 8 that V_{ps} rises slowly (approximately logarithmically) on increase in I_c . On the other hand, the value of V_{ps} corresponding to a fixed I_c depends quite strongly on temperature. In the investigated temperature range the dependence $\Delta(T)$ is weak. The existence of a strong dependence of V_{ps} on T is a demonstration of the important role played by thermal effects in the phase slip mechanism.

Phase slip centers have been investigated theoretically and experimentally for a fairly long time in narrow superconducting channels at a temperature close to the superconducting transition.²⁸ Since in the case of a coherent CDW, as in the case of superconductivity, we are dealing with the "collectivized" motion of electrons and with a phase which depends on the coordinates and time, the analogy between these two systems is quite good. In both cases the appearance of a phase slip center, i.e., of a momentary departure from coherence, is due to the need to get rid of spatial and temporal increases in the phase above permissible values.

In the case of a Peierls conductor with a coherent CDW a homogeneous tension in the CDW (due to variation of temperature) or an inhomogeneous strain in the CDW (in an electric field) is retained until the relief of these strains becomes more favorable through the appearance (or disappearance) of a new CDW period. Then, the energy gap should vanish in a certain local region of a sample,²³ the phase coherence to the left and right of this region should be lost, and the phase should be rotated by an amount which is a

multiple of 2π , which restores a state with an undeformed CDW. The process may then be repeated cyclically.

For a CDW to be destroyed and Δ to vanish in a local region in a sample requires a certain energy F , which represents the energetic barrier against the formation of a phase slip center and appearance of a new CDW period. The application of a voltage V_{ps} to such a barrier reduces its effective height by $\sim \eta V_{ps}$, where η is the charge flowing due to the slip of the phase by 2π . At a sufficiently high temperature there is a finite probability of overcoming this barrier because of thermodynamic fluctuations and due to the electric field^{28,29}:

$$I_c = I_0 e^{-F/T} \text{sh}(\eta V_{ps}/2T). \quad (10)$$

The continuous curves in Fig. 8 are the dependences calculated using the above formula on the assumption that $I_0 = 3.5$ A, $F = 2500$ K, $\eta = 60e$, where e is the electron charge. We can see from Fig. 8 that the experimental results obtained for small TaS₃ samples are described fairly satisfactorily by Eq. (10) throughout the investigated temperature range.

The values of the parameter η/e deduced from five relations $V_{ps}(I_c)$, representing sections of different length in three samples ($T = 120$ K), lie within the range 30–80. The energy barrier per electron (on the order of the condensation energy per electron) is eF/η and can be obtained by extrapolation of the dependence $V_{ps}(I_c)$ plotted for a certain fixed current I_c , to $T = 0$. In the case of three samples investigated the value of eF/η lies within the range 4–6 meV (~ 40 – 60 K). The ratio $\eta/e = 60$ is the number of electrons which cross a region with a phase slip center when a new CDW period appears. Hence, we can estimate the volume of the sample where a phase slip center appears: $v_{ps} = \eta/en$, where n is the carrier density. Substituting in TaS₃ the value $n \approx 10^{21} \text{ cm}^{-3}$ (Ref. 26), we obtain $v_{ps} = 6 \times 10^{-20} \text{ cm}^{-3}$, which is of the order of ξ^3 . This means that the destruction of a CDW and the suppression of the gap occur in a volume $\sim \xi^3$, as expected in the case of formation of a time-dependent amplitude soliton.²³

A phase slip center (v_{ps}/λ) occupies approximately 10^{-3} of the area of the investigated samples and if a single phase slip center were present in the cross section it would be impossible to observe steps in the $R(T)$ curve due to such a center. Hence, it follows that any phase slip process occurs either due to the presence of many slip centers in the cross section of a sample^{27,29} or the process of dephasing of a CDW, which begins in a small part of the cross section of a sample (as a seed), spreads over the whole cross section because of phase coherence. The latter hypothesis is clearly supported by the observation that the spectrum of narrow-band oscillations in samples with small cross section consists of a single narrow line and its harmonics.

IV. CONCLUSIONS

These experimental results demonstrate that a coherent CDW appears in small TaS₃ samples. They also make clear the major role played by stresses and strains in a CDW, which shift the chemical potential level, make it dependent on the spatial coordinates, and finally give rise to a phase slip center.

These results and calculations, taken together with the

theoretical investigations^{23,28} and the analogy with phase slip in superconducting channels,²⁸ make it possible to suggest the following qualitative description of the effects which occur in small TaS₃ samples with a coherent CDW. At a given temperature a CDW is in some state governed by its previous electrical and thermal history, by the pinning effects, and by the boundary conditions. This state is characterized by a specific distribution of the wave vector $q(x)$ of a CDW (in the case of small samples we can expect a set of discrete states $q \approx q_m = 2\pi/L$) and by an associated, in accordance with Eq. (2), spatial distribution of the chemical potential $\zeta(x)$, which is a measure of the tension in a CDW.

Relief of the excess tension in a CDW may result from transitions between such states stimulated by the thermally activated process of phase slip. The frequency of transitions between different states is proportional to $\exp(-F/T)$, where F is the energy barrier between these states which—according to our experimental results—is fairly large, satisfying $F > 10^3$ K at $T = 120$ K. It is important to note that the stresses and strains in a CDW increase the energy stored by the electron system in a Peierls conductor and thus reduce the effective height of the energy barrier.

At high temperatures, when $T_p - T \ll T_p$ and the height of the barrier (related to the condensation energy Δ) can in principle be small because of reduction in Δ , transitions between different states are quite readily activated in both directions, the lifetime of metastable states is short, and the dependence $R(T)$ is practically free of hysteresis and discontinuities. Cooling reduces the probability of overcoming the barrier, the frequency of transitions accompanied by the formation of phase slip centers decreases strongly, and the lifetime of metastable states as well as their role increase. Temperature cycling gives rise to hysteresis in the dependence $R(T)$. A barrier can be overcome at low temperatures by stronger strains and by deviation of a CDW from equilibrium, the temperature interval between the steps becomes greater, and discrete states in small samples seem to become superimposed on one another (Fig. 2).

The application of an external electric field lowers the barrier height and enhances the unidirectional nature of transitions across the barrier. This case corresponds to steps of the $R_d(I)$ curve, observed for our samples when the number of phase slip centers is finite, when the residual thermal strains are relieved (curve 1 in Fig. 4c), and it also corresponds to steps observed during the cycling of the current ($I < I_T$) (Figs. 4b and 4c). In the case of large samples with a very large number of phase slip centers these dependences are smooth and free of steps (Fig. 4a). When the current exceeds a certain threshold value, so that a CDW tends to propagate as a whole and the process of phase slip at the contacts ensures the motion of a CDW, the influence of the electric field becomes strong. The transition frequency begins to depend strongly also on the voltage, proportionally to $\sinh(\eta V_{ps}/2T)$.

For $I - I_T \ll I_T$, an important role is played by spontaneous irregular formation of phase slip centers, which corresponds to nonperiodic low-frequency noise oscillations of the voltage at the moment of formation of a phase slip center.^{32,33} A further increase in the voltage effectively reduces the barrier and the formation of phase slip centers begins to be governed largely by the applied electric field. Phase slip

then becomes a regular periodic process which in the case of small samples corresponds to an oscillation spectrum consisting of separate narrow lines (Fig. 6c). In the case of large samples the number of phase slip centers can also be large and the oscillation spectrum has many lines with different structures and widths (Figs. 6a and 6b).

Clearly, the above model can account also for a number of other phenomena. For example, the rise of the threshold field and the reduction in the contribution of a CDW to the conduction process in fields $E > E_T$ during cooling,² observed for many quasi-one-dimensional materials, may be attributed to a considerable [proportional to $\exp(-F/T)$] reduction in the probability and frequency of transitions across a barrier in the phase slip process. We cannot exclude the possibility that if $T \ll F$, we may encounter—in addition to the above-barrier transitions—also tunneling through a barrier, and the current-voltage characteristics can be of the form typical of such processes, with an electric-field-dependent activation energy of conduction in the range $E > E_T$ (Ref. 12). Short-lived conversion of electrons condensed in a CDW to a normal state, which is necessary for phase slip and occurs in the specific case when $V_{ps} \gtrsim E_c L$ (Fig. 7), may also be the reason for the observed scaling between the ohmic conductivity ($E < E_T$) and the differential conductivity when $E > E_T$ (Ref. 33). It should also be pointed out that the appearance of stresses and strains in this wave is less likely in a commensurate CDW and the effects discussed above and associated with the strains in CDW and with phase slip centers may not occur, as confirmed by the experimental results reported in Ref. 34.

The authors are grateful to Ya. S. Savitskaya for supplying TaS₃ samples and to S.A. Brazovskii and V. Ya. Pokrovskii for discussing the results.

¹The authors are grateful to A.B. Ormont for carrying out the electron-microscopic measurements.

¹*Charge Density Waves in Solids* (Proc. Intern. Conf. Budapest, 1984 ed. by G. Hutiray and J. Solyom), Springer Verlag, Berlin (1985) [Lecture Notes in Physics, Vol. 217].

²P. Monceau, in: *Electronic Properties of Inorganic Quasi-One-Dimensional Compounds* (ed. by P. Monceau), Part 2, Experimental, D. Reidel, Dordrecht, Netherlands (1985), p. 139.

³R. P. Hall and A. Zett Solid State Commun. **50**, 813 (1984).

⁴D. V. Borodin, S. V. Zaitsev-Zotov, and F. Ya. Nad', Zh. Eksp. Teor. Fiz. **90**, 318 (1986) [Sov. Phys. JETP **63**, 184 (1986)].

⁵G. Hutiray, G. Mihaly, and L. Mihaly, Solid State Commun. **47**, 121 (1983).

⁶K. B. Efetov and A.I. Larkin, Zh. Eksp. Teor. Fiz. **72**, 2350 (1977) [Sov. Phys. JETP **45**, 1236 (1977)].

⁷H. Fukuyama and P. A. Lee, Phys. Rev. B **17**, 535 (1978); P.A. Lee and T.M. Rice, Phys. Rev. B **19**, 3970 (1979).

⁸L. Mihaly and G. Gruner, Solid State Commun. **50**, 807 (1984).

⁹C. H. Chen and R. M. Fleming, Solid State Commun. **48**, 777 (1983).

¹⁰D. V. Borodin, S. V. Zaitsev-Zotov, and F. Ya. Nad', Pis'ma Zh. Eksp. Teor. Fiz. **43**, 485 (1986) [JETP Lett. **43**, 625 (1986)].

¹¹D. V. Borodin, S.V. Zaitsev-Zotov, and F. Ya. Nad', Preprint No. 4(443) [in Russian], Institute of Radio Engineering and Electronics, Academy of Sciences of the USSR, Moscow (1986).

¹²F. Ya. Nad', in: *Charge Density Waves in Solids* (Proc. Intern. Conf. Budapest, 1984, ed. by G. Hutiray and J. Solyom) Springer Verlag, Berlin (1985), p. 286 [Lecture Notes in Physics, Vol. 217].

¹³A. W. Higgs and J.C. Gill, Solid State Commun. **47**, 737 (1983).

¹⁴D. S. Fisher, Phys. Rev. Lett. **50**, 1486 (1983).

¹⁵M. O. Robbins and R.A. Klemm, Phys. Rev. B **34**, 8496 (1986).

¹⁶S. K. Zhilinskii, M. E. Itkis, I. Yu. Kal'nova, F. Ya. Nad', and V. B. Preobrazhenskii, Zh. Eksp. Teor. Fiz. **85**, 362 (1983) [Sov. Phys. JETP **58**, 211 (1983)].

- ¹⁷D. V. Borodin, S. V. Zaitsev-Zotov, and F. Ya. Nad', Pis'ma Zh. Eksp. Teor. Fiz. **41**, 340 (1985) [JETP Lett. **41**, 416 (1985)].
- ¹⁸P. Monceau, J. Richard, and M. Renard, Phys. Rev. B **25**, 931 (1982).
- ¹⁹Z. Z. Wang, H. Salva, P. Monceau, M. Renard, C. Roucau, R. Ayroles, F. Levy, L. Guemas, and A. Meerschaut, J. Phys. Lett. **44**, L311 (1983).
- ²⁰T. Tamegai, K. Tsutsumi, S. Kagoshima, Y. Kanai, M. Tani, H. Tomozawa, M. Sato, K. Tsuji, J. Harada, M. Sakata, and T. Nakajima, Solid State Commun. **51**, 585 (1984).
- ²¹S. N. Artemenko and A. F. Volkov, Zh. Eksp. Teor. Fiz. **81**, 1872 (1981) [Sov. Phys. JETP **54**, 992 (1981)].
- ²²M. E. Itkis, F. Ya. Nad', and V. Ya. Pokrovskii, Zh. Eksp. Teor. Fiz. **90**, 307 (1986) [Sov. Phys. JETP **63**, 177 (1986)].
- ²³S. N. Artemenko, A. F. Volkov, and A. N. Kruglov, Zh. Eksp. Teor. Fiz. **91**, 1536 (1986) [Sov. Phys. JETP **64**, 906 (1986)].
- ²⁴L. P. Gor'kov, Pis'ma Zh. Eksp. Teor. Fiz. **38**, 76 (1983) [JETP Lett. **38**, 87 (1983)]; Zh. Eksp. Teor. Fiz. **86**, 1818 (1984) [Sov. Phys. JETP **59**, 1057 (1984)].
- ²⁵B. Fisher, Solid State Commun. **46**, 227 (1983); A. W. Higgs, in: *Charge Density Waves in Solids* (Proc. Intern. Conf., Budapest, 1984, ed. by G. Hutiray and J. Solyom), Springer Verlag, Berlin (1985), p. 422 [Lecture Notes in Physics, Vol. 217].
- ²⁶Yu. I. Latyshev, Ya. S. Savitskaya, and V. V. Frolov, Pis'ma Zh. Eksp. Teor. Fiz. **38**, 446 (1983) [JETP Lett. **38**, 541 (1983)].
- ²⁷N. P. Ong and G. Verma, Phys. Rev. B **27**, 4495 (1983); N. P. Ong, G. Verma, and K. Maki, Phys. Rev. Lett. **52**, 663 (1984).
- ²⁸B. I. Ivlev and N. B. Kopnin, Usp. Fiz. Nauk **142**, 435 (1984) [Sov. Phys. Usp. **27**, 206 (1984)].
- ²⁹J. C. Gill, J. Phys. C **19**, 6589 (1986).
- ³⁰J. C. Gill, Solid State Commun. **44**, 1041 (1982); in: *Charge Density Waves in Solids* (Proc. Intern. Conf., Budapest, 1984, ed. by G. Hutiray and J. Solyom), Springer Verlag, Berlin (1985), p. 377 [Lecture Notes in Physics, Vol. 217].
- ³¹G. Mihaly, G. Hutiray, and L. Mihaly, Phys. Rev. B **28**, 4896 (1983).
- ³²J. C. Gill and A. W. Higgs, Solid State Commun. **48**, 709 (1983).
- ³³N. P. Ong, C. B. Kalem, and J. C. Eckert, Phys. Rev. B **30**, 2902 (1985).
- ³⁴V. B. Preobrazhenskii (Preobrazhensky), A. N. Taldenkov, and S. Yu. Shabanov, Solid State Commun. **54**, 399 (1985).

Translated by A. Tybulewicz